Science of the Total Environment 915 (2024) 170255

Contents lists available at ScienceDirect

Science of the Total Environment

journal homepage: www.elsevier.com/locate/scitotenv

Trade-off of ecosystem productivity and water use related to afforestation in southcentral USA under climate change

Tian Zhang [a,*,1], Jia Yang [a], Abigail Winrich [b], Rodney E. Will [a], Chris B. Zou [a]

[a] *Department of Natural Resource Ecology and Management, Oklahoma State University, Stillwater, OK 74078, USA*
[b] *Department of Civil and Environmental Engineering, Oklahoma State University, Stillwater, OK 74078, USA*

HIGHLIGHTS

- SWAT+ was used to simulate afforestation impact on productivity and water use.
- Increasing tree cover boosts carbon sequestration and water use efficiency.
- Extensive tree cover reduces water yield, particularly in warmer, drier climates.
- The development of afforestation policy should consider both carbon and water.

GRAPHICAL ABSTRACT

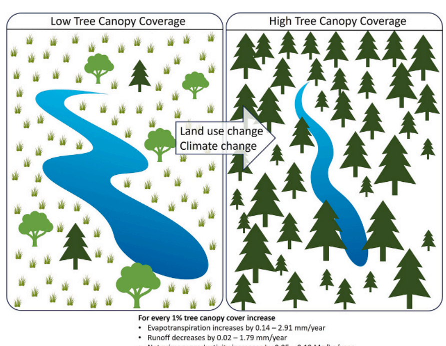

ARTICLE INFO

Editor: Fernando A.L. Pacheco

Keywords:
SWAT+
Tree cover increase
Southern Great Plains
RCP45 and RCP85
Climate transition zone

ABSTRACT

The increase of tree canopy cover due to woody plant encroachment and tree plantations modifies both carbon and water dynamics. The tradeoffs between ecosystem net primary productivity (NPP) and water use with increasing tree cover in different climate conditions, particularly under future climate scenarios, are not well understood. Within the climate transition zone of the southern Great Plains, USA, we used the Soil and Water Assessment Tool+ (SWAT+) to investigate the combined impacts of increasing tree cover and climate change on carbon and water dynamics in three watersheds representing semiarid, subhumid, and humid climates. Model simulations incorporated two land use modifications (Baseline: existing tree cover; Forest +: increasing evergreen tree cover), in conjunction with two climate change projections (the RCP45 and the RCP85), spanning two time periods (historic: 1991–2020; future: 2070–2099). With climate change, the subhumid and humid watersheds exhibited a greater increase in evapotranspiration (ET) and a corresponding reduction in runoff compared to the semi-arid watershed, while the semi-arid and subhumid watersheds encountered pronounced losses in water availability for streams (>200 mm/year) due to increasing tree cover and climate change. With every 1 % increase in tree cover, both NPP and water use efficiency were projected to increase in all three watersheds under both climate change scenarios, with the subhumid watershed demonstrating the largest increases (>0.16 Mg/ha/year and 170 %, respectively). Increasing tree cover within grasslands, either through woody plant expansion or afforestation, boosts ecosystem NPP, particularly in subhumid regions. Nevertheless, this comes with a notable

* Corresponding author.
E-mail address: tian.zhang@okstate.edu (T. Zhang).
[1] Postal address: 008C Ag Hall, Oklahoma State University, Stillwater, OK 74078, USA.

https://doi.org/10.1016/j.scitotenv.2024.170255
Received 21 November 2023; Received in revised form 10 January 2024; Accepted 16 January 2024
Available online 19 January 2024

decrease in water resources, a concern made worse by future climate change. While afforestation offers the potential for greater NPP, it also brings heightened water scarcity concerns, highlighting the importance of tailoring carbon sequestration strategies within specific regions to mitigate unintended repercussions on water availability.

1. Introduction

Human activities over the past decades have been leading to climate warming (Masson-Delmotte et al., 2021; Lal, 2008) and reduced global forest coverage (Zhang and Wei, 2021). Afforestation and reforestation are widely recognized as a nature-based solution to mitigate climate change and resultant hydrometeorological hazards (Chausson et al., 2020; Di Sacco et al., 2021). Increasing tree cover in understocked forests could potentially boost ecosystem carbon sequestration capacity by approximately 20 % in the USA (Domke et al., 2020), and afforestation on a quarter of the agricultural land in the midwestern USA could increase carbon sequestration substantially. The increase would be equivalent to 6 % - 8 % of CO_2 emissions in the region over the next 50 years (Niu and Duiker, 2006). Clearly, increasing woody vegetation cover in rangelands to enhance carbon sequestration is alluring, given their extensive distribution (Morgan et al., 2010; Nosetto et al., 2006), but this would also compromise many ecosystem services related to grasslands and savannas.

Along with the introduction of cattle and cattle grazing systems in the past 160 years, tree cover has increased substantially in the southern Great Plains (SGP) of the USA, especially in the past half-century (Archer et al., 1995; Kulmatiski and Beard, 2013; Van Auken, 2009). In Texas rangelands, woody cover has increased multiple times during the past decades (Ansley et al., 2001; Asner et al., 2003), primarily from the expansion of honey mesquite (*Prosopis glandulosa*). Towards the north of the SGP, the woody cover in rangeland has rapidly increased due to the riparian expansion (Wine and Zou, 2012) and woody encroachment in uplands, primarily by a juniper species (*Juniperus virginiana*, eastern redcedar) (Briggs et al., 2002; Wang et al., 2017).

While the major land use in SGP is rangeland, characterized by grasses, forbs, or shrubs suitable for grazing and browsing use (Bigelow and Borchers, 2017), tree plantations in the SGP have a long history, dating back to the early days of European-American settlement. In the 19th century, trees were sparsely planted for a variety of purposes, including providing shade, windbreaks, and timber (Gardner, 2009). Apart from the Great Plains Shelterbelt project in the 1930s and the continuous experiments at Nebraska National Forest since the early 20th century in the northern Great Plains, there were no large-scale tree plantations in the SGP in recent decades. Studies conducted in the northern Great Plains reported that conifer plantations and eastern redcedar encroachment led to greater evapotranspiration (ET, the process of moving water from the Earth's surface into the atmosphere, including evaporation and transpiration) and reduced soil moisture and streamflow (Adane et al., 2018; Kishawi et al., 2023). However, the temptation to plant trees in the SGP is on the rise, due to its abundant land, warmer climate, and a growing awareness of the benefits of trees. Trees are especially favored for their capacity to sequester large quantities of atmospheric carbon into their biomass as a method to mitigate carbon emissions and combat climate change (Sauer et al., 2023).

An increase in tree cover whether it occurs naturally or from planting is widely reported to increase net primary productivity (NPP, the net gain of biomass retained in an ecosystem) and standing biomass (Eldridge et al., 2011; Potts et al., 2006; Ameray et al., 2021). Barger et al. (2011) pointed out that land conversion from grassland to woodland increased the aboveground net primary productivity (ANPP) by 0.7 g C/m^2/year with every 1 mm increase in mean annual precipitation (MAP) in semi-arid areas where MAP is >336 mm. Meanwhile, this increased tree cover will influence the water balance due to greater ET (Joffre and Rambal, 1993; Zhang et al., 1999; Zou et al., 2014). ET is commonly characterized as green water flow, emphasizing its association with soil moisture and its utilization by plants, and the streamflow and groundwater recharge are often referred to as blue water flow, underscoring their connection to liquid water that is extractable and managed for diverse human activities (Falkenmark, 1995). In this study, blue water flow is used interchangeably with watershed water yield and water resource availability. Conceptually, there is a trade-off between increasing NPP and blue water flow with the progression of woody plant expansion in the SGP because of larger leaf area generating more gas exchange. In the past decades, several studies investigated the impact of increasing tree cover by woody plant encroachment (WPE) on blue water flow in the SGP (Huxman et al., 2005; Wilcox and Huang, 2010; Starks and Moriasi, 2017; Zou et al., 2018). These studies generally found an increase in ecosystem water use, i.e., green water flow, and a reduction in blue water flow as woody cover increases.

In terms of afforestation through tree planting, studies conducted across various spatial scales and climate regions concluded that increasing tree cover often contributes to a decrease in blue water due to a rise in ET (Schwärzel et al., 2020; Tölgyesi et al., 2023). In addition, afforestation causes an increase in net-absorbed radiation and localized surface warming as a result of the decrease in albedo (Bonan, 2008), especially in higher latitudes (Bala et al., 2007; Mykleby et al., 2017). Notably, the effectiveness of afforestation in temperate regions to mitigate global warming is still debatable due to the cross-continental transport of water vapor caused by atmospheric circulations (Bala et al., 2007; Hoek van Dijke et al., 2022).

There is a lack of studies that compiled data on both carbon gain and water loss in tree plantations in the SGP. Studies on individual components showed increased vegetation water usage and while topsoil organic carbon increased, it was found to decrease deeper in soil after conifer species encroached within the stands (Torquato et al., 2020) and compared to nearby grassland (Li et al., 2023). Despite the increasing interest in plantation and climate change mitigation, there is still a lack of understanding regarding how increasing tree canopy cover, climate conditions, and climate change will interact to affect the NPP potential, ET, and water resource sustainability in this region. This is crucial given that tree planting programs usually require a long-term commitment meaning future climate must be considered for ecohydrological evaluation so that green and blue water trade-offs can be properly addressed (Di Sacco et al., 2021; Tölgyesi et al., 2023).

The Soil and Water Assessment Tool (SWAT) model is widely used to simulate the ecological and hydrological impacts across diverse spatiotemporal scales under various climate and land use conditions (Abbaspour et al., 2015; Qiao et al., 2022). For that reason, this study employed the SWAT+ model to examine the impacts of increasing tree canopy cover and climate change on water balance and NPP of three watersheds in semiarid, subhumid, and humid climates along the climate transition zone in the SGP, USA. We hypothesized that: 1) both increasing tree cover and future climate change will increase vegetation water uptake and reduce water yield; 2) increasing tree cover will enhance NPP with a larger gain in the humid climate than in the drier climate; and 3) the capacity of NPP associated with tree cover increase will decrease in future climate.

2. Study sites and methods

2.1. Study sites

Three watersheds representing different climate conditions were selected within the climate transition zone of the SGP, USA (Fig. 1a and b). The upper Washita River watershed (Washita, 3527 km^2, Fig. S1) is located in the semiarid region in the west of our study domain across the High Plains and the Western Redbed Plains (mean elevation 694 m) and the natural vegetation is mixed prairie with predominant soil series associations of Woodward-Quinlan (29.5 %), Nobscot-Devol-Delwin (18.1 %), and Mansic-Irene-Acuff (11.9 %). The Black Bear Creek watershed (BBear, 1355 km^2, Fig. S2) is located in the subhumid Cross Timbers ecoregion across the Central Redbed Plains and the Northern Limestone Cuesta Plains (mean elevation 321 m) and the natural vegetation is a mosaic of tallgrass prairie and oak woodland with predominant soil series associations of Zaneis-Renfrow-Grainola-Coyle (29.6 %), Renfrow-Kirkland-Grainola (29.3 %), and Yahola-Pulaski-Port-Ashport (12.4 %). The Kiamichi River watershed (Kiamichi, 2820 km^2, Fig. S3) is located in the east of the study domain across the Ridge and Valley Belt (mean elevation 284 m) of the Ouachita Highlands and is a humid forested watershed with predominant soil series associations of Sherless-Pirum-Clebit-Carnasaw (55.1 %), Wister-Tuskahoma-Sobol-Neff (16.4 %), and Tuskahoma-Pickens-Clebit (14.1 %) (Tyrl et al., 2007). The mean annual temperatures (MAT) range from 7.4 to 22.3 °C for Washita, 9.0 to 22.2 °C for BBear, and 9.9 to 22.7 °C for Kiamichi (Fig. 1b), while the mean annual precipitations (MAP) are 621.7 mm for Washita, 923.9 mm for BBear, and 1328.4 mm for Kiamichi (Fig. 1c). The dominant land conditions in Washita included rangeland (88.3 %) and agricultural land (9.2 %); in BBear, it was rangeland (57.4 %), agricultural land (30.2 %), and forest (8.7 %); and in Kiamichi, it was forest (74 %) and rangeland (21.5 %). Among all three watersheds, only the west half of Washita is located above one of the principal aquifers, High Plains aquifer (Ogallala aquifer, USGS, 2003).

2.2. Model setup and scenario descriptions

The SWAT+ (Soil and Water Assessment Tool+) is an open-sourced and semi-distributed hydrological model developed to predict the long-term impacts of land management on water, sediment, and chemical yield in watersheds with different sizes, soils, land use types, and management conditions (Arnold and Fohrer, 2005; also see Bieger et al., 2017). In this study, we used SWAT+ (SWAT rev 60.5.7) to conduct simulations at a watershed scale. Watersheds were delineated by QSWAT+ 2.4.0 in QGIS 3.22.9 (QGIS.org, London, UK). Input data include Shuttle Radar Topography Mission (SRTM) DEM (Farr et al., 2007), National Land Cover Database (NLCD) (Homer et al., 2004),

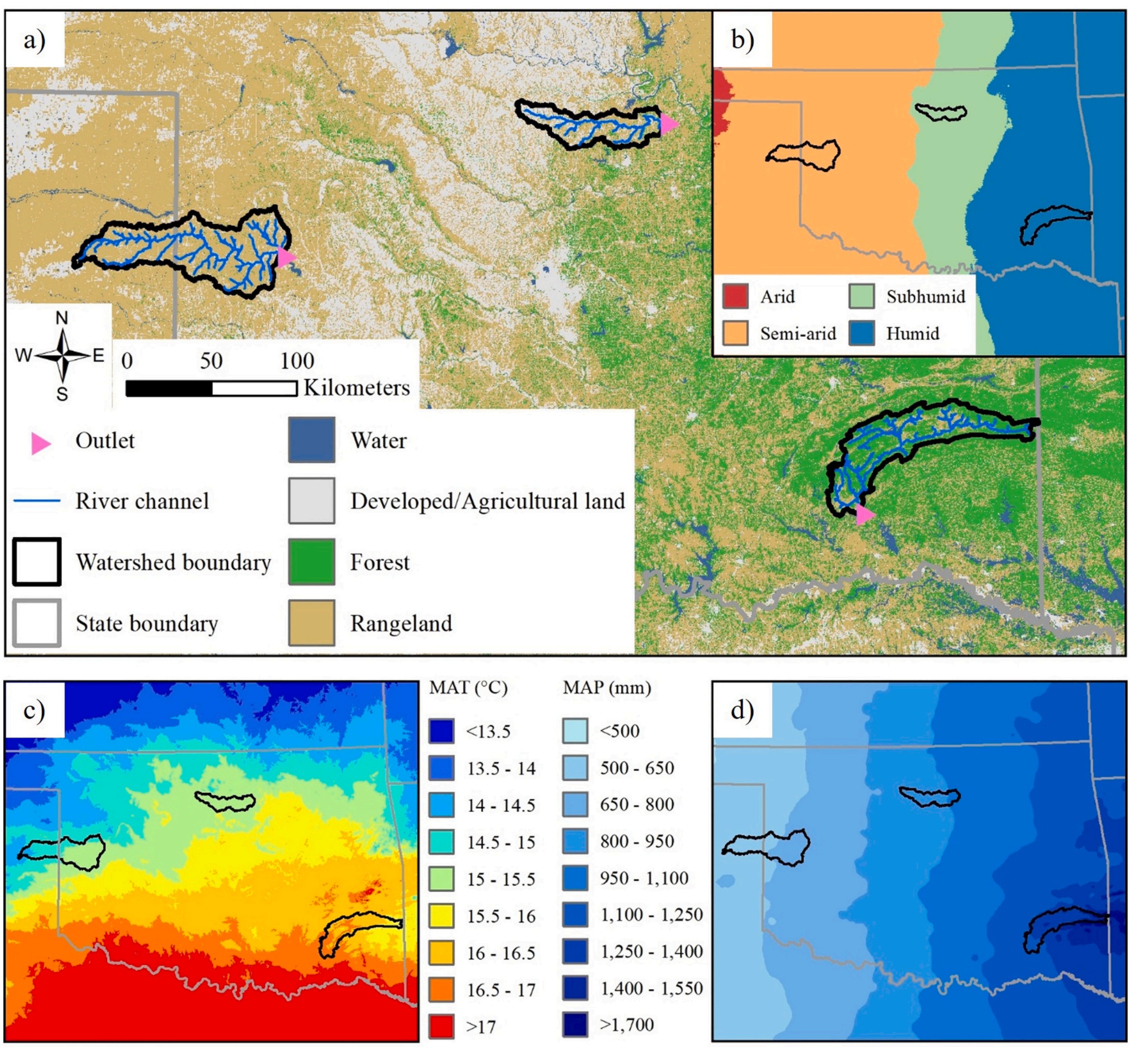

Fig. 1. Study areas of the Washita River watershed (Washita, left), the Black Bear Creek watershed (BBear, middle), and the Kiamichi River watershed (Kiamichi, right) (a). The land use/land cover type dataset was retrieved from the National Land Cover Dataset (NLCD). Watershed boundary and river channels were derived from the Shuttle Radar Topography Mission (SRTM) digital elevation data. Climate region (b) data was retrieved from the Global Aridity Index and Potential Evapotranspiration Database – Version 3 (Global-AI_PET_v3) (Zomer et al., 2022). Data from PRISM Climate Group were used to produce long-term (1991–2020) mean annual temperature (c) and mean annual precipitation (d).

gridMET historic climate data (Abatzoglou, 2013), future climate data simulated by Community Climate System Model (CCSM4) under the Representative Concentration Pathway RCP45 and RCP85 (Gent et al., 2011), and State Soil Geographic (STATSGO2). All the input data were projected to the Transverse Mercator UTM Zone 14 N projection coordinate system. Then they were resampled to a spatial resolution of 90 m using the bilinear resampling technique for DEM and the majority resampling technique for NLCD and STATSGO2 to ensure data compatibility.

The CCSM4 was developed by the University Corporation for Atmospheric Research (UCAR), which is a coupled general circulation model (GCM, Gent et al., 2011). It included the Community Atmosphere Model, Community Land Model, Parallel Ocean Program, and Community Sea Ice Model. In this study, we chose the RCP45 and RCP85 scenarios from the Intergovernmental Panel on Climate Change (IPCC). RCP45 is an intermediate scenario in greenhouse gas emissions and climate change, while RCP85 is considered the worst-case scenario and the emission continues to rise in the 21st century.

The study incorporated two land use conditions (Baseline: existing tree cover; Forest +: increasing tree cover), two diverse climate change projections (low emission: RCP45; high emission: RCP85), two time spans (historic: 1991–2020; future: 2070–2099), resulting in 8 unique scenarios for each watershed and 24 model runs total (2 land use conditions × 2 climate projections × 2 time spans × 3 watersheds). ET, runoff (the quantity of water discharged in surface streams), and NPP were estimated in each of the 24 model runs. For historic climate scenarios, the climate input data were infused by gridMET data and CCSM4 RCP45/RCP85 modeled data to ensure data consistency and for the future period from 2070 to 2099, solely CCSM4 RCP45/RCP85 modeled data were input. For Forest+, we reclassified all rangeland and forest as evergreen forest (FRSE) using ArcGIS Pro 3.0.1 (ESRI, Redlands, CA, USA) to resemble the ongoing juniper encroachment or potential conifer plantation under all time periods and climate scenarios (Table 1).

2.3. Model calibration and validation

SWAT+ was used to make hydrological simulations in the three watersheds in 1991–2020 with gridMET meteorological data. A five-year period, 1991–1995, was used for model warm-up to sufficiently minimize the effects of initial state variables on model outputs. The period of 1996–2010 was used for model calibration and 2011–2020 was used for model validation. Model calibration was done using SWAT+ Toolbox (v1.0.5) with USGS river discharge data – USGS 07324200 near Hammon, OK (35.66° N, 99.31° W) for Washita, USGS 07153000 near Pawnee, OK (36.34° N, 96.80° W) for BBear, and USGS 07336200 near Antlers, OK (34.25° N, 95.61° W) for Kiamichi. Table 2 shows the list of parameters used in the calibration process identified by the dynamically dimensioned search algorithm and their optimal values.

According to Moriasi et al. (2007), if NSE (Nash-Sutcliffe efficiency), PBIAS (percent bias), and RSR (RMSE-observations standard deviation ratio) were > 0.5, <5 %, and < 0.7, respectively, the model performance is between satisfactory and very good. Negative PBIAS values indicate an overestimate, while positive PBIAS values indicate an underestimate. So, there was a slight overestimate of monthly discharge in BBear and Kiamichi (Fig. 2). NSE values decreased from the humid region to the arid region, which is discussed in Section 4.2.

Table 1
Percentage of grassland and forest coverage in Washita, BBear, and Kiamichi. Baseline represented the current vegetation conditions. Forest+ indicated the scenarios of increasing evergreen tree cover. The remaining lands not counted as forest under the Forest+ scenarios are agricultural or developed.

	Washita		BBear		Kiamichi	
Land use	Baseline	Forest+	Baseline	Forest+	Baseline	Forest+
Grassland	61.6	0	49.5	0	21.5	0
Forest	1.2	62.8	13.1	62.6	74.0	95.5

Table 2
List of parameter optimal values identified using the dynamically dimensioned search algorithm. Dashed lines represent parameters that were not calibrated.

Parameter names	Optimal values for Washita	Optimal values for BBear	Optimal values for Kiamichi
v_EPCO* (plant uptake compensation factor)	16.51	18.63	0.88
v_ESCO (soil evaporation compensation factor)	−15.95	25.31	0.56
a_CN2* (curve number)	8.18	−89.37	7
v_ALPHA (baseflow alpha factor)	–	–	0.29
v_AWC (available water capacity)	−3.49	33.88	1.02
r_FLO_MIN* (minimum aquifer storage to allow return flow)	48.63	39.69	300
v_REVAP_CO (groundwater revap coefficient)	−13.72	33.14	0.08
r_REVAP_MIN (threshold depth of water in the shallow aquifer for revap)	147.27	−94.73	100
v_CANMX (maximum canopy storage)	1.19	12.50	6.1
v_SLOPE_LEN (slope length for erosion)	36.52	34.01	21.44
v_LAT_TTIME (lateral flow travel time)	15.97	83.51	3.09
v_SNOFALL_TMP (snowfall temperature)	−9.92	2.20	0.64
v_SNOMELT_TMP (snow melt base temperature)	−9.41	−7.75	1.52
v_SNOMELT_MAX (snow melt maximum temperature)	9.13	7.84	4.36
v_SNOMELT_MIN (snow melt minimum temperature)	−9.08	−4.79	1.55
v_SNOMELT_LAG (snow melt lag time)	5.53	7.35	0.8
a_BD (bulk density)	−77.05	−83.63	–
a_PERCO (percolation coefficient)	377.46	−72.79	100
a_SURLAG (surface runoff lag coefficient)	2.02	33.42	–

* v: replaced with the optimal value. a: increased by the optimal value. r: multiplied by the optimal value. For example, if the original value is 100, +3 % change means 100 + 100 * 3 % = 103.

2.4. Result analyses

Ecosystem water use efficiency (WUE) was calculated using the ratio of NPP to ET to reflect the biomass growth (kg) for a given area (ha) per unit ET (mm) (kg/ha/mm). The differences in ET, runoff, blue water depth, NPP, and WUE between baseline and Forest+ scenarios in each time period and climate scenario were calculated for each 1 % increase in forest cover of the total watershed area for each watershed.

3. Results

3.1. Future climate

During the two time periods of 1991–2020 and 2070–2099, both MAT and MAP decreased from east to west, i.e., greatest in the humid Kiamichi watershed to lowest in the semi-arid Washita watershed. CCSM4 projected an average increase of 2.3 °C and 4.1 °C in MAT, but an average decrease of 32.7 mm and 36.7 mm in MAP in the three watersheds under the RCP45 and the RCP85, respectively (Table 3). The model projected that Kiamichi would have about 8.2 mm more annual rainfall in the late 21st century compared to 1991–2020 under the RCP85. Excluding this increase, Washita and BBear had an average of 59.2 mm decrease in MAP comparing 1991–2020 to 2070–2099 under RCP85, compared to only a 37.1 mm decrease under RCP45.

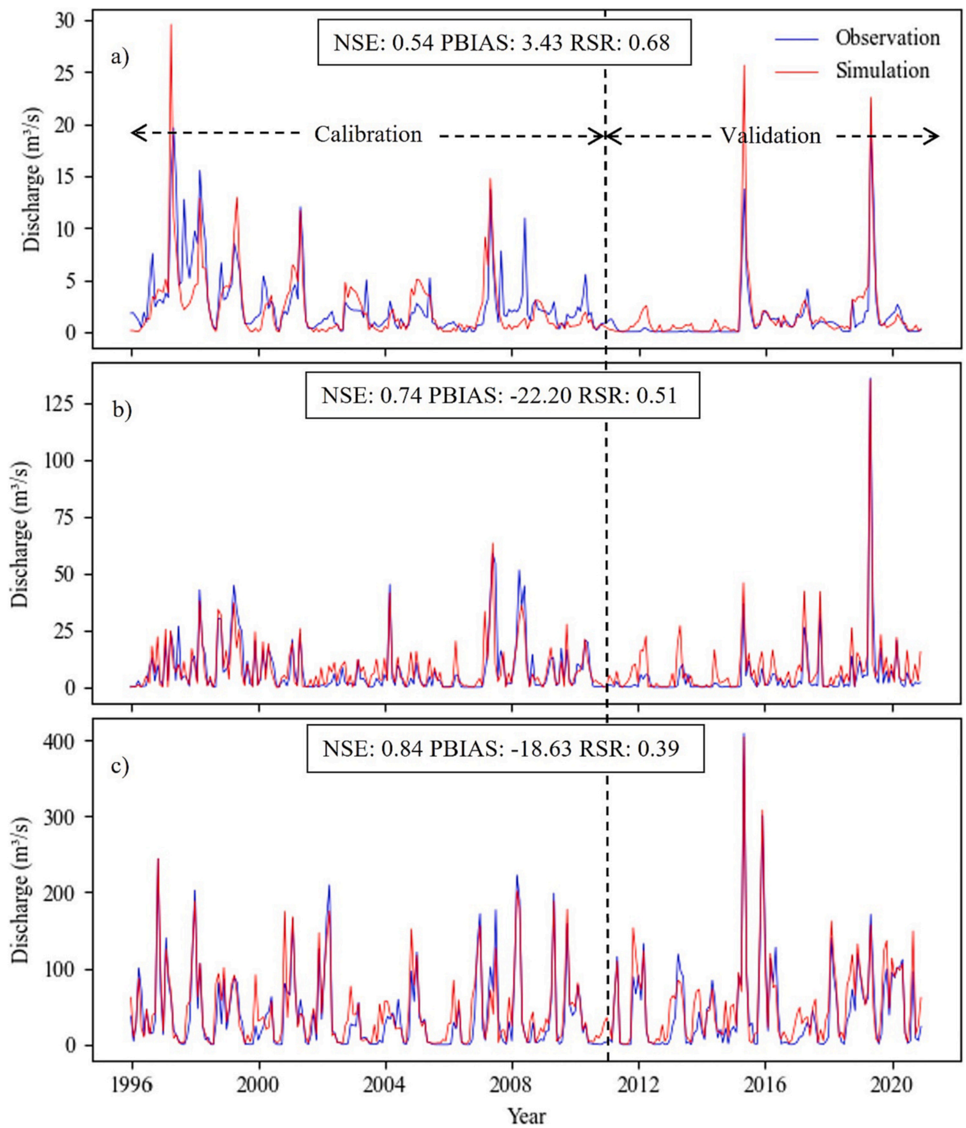

Fig. 2. Comparison between monthly mean river discharge data simulated by SWAT+ (red) and USGS observed data (blue) of Washita (a), BBear (b), and Kiamichi (c). Statistics of Nash–Sutcliffe efficiency (NSE), percent bias (PBIAS), and RMSE-observations standard deviation ratio (RSR) for both the calibration and validation periods in each panel.

Table 3
Mean annual temperature (MAT) and mean annual precipitation (MAP) projected by CCSM4 under the RCP45 and the RCP85 for Washita, BBear, and Kiamichi watersheds, respectively. Values after ± symbol represent standard deviations, denoting annual variability for the entire simulated period.

		RCP45		RCP85	
		1991–2020	2070–2099	1991–2020	2070–2099
MAT	Washita	15.5 ± 1.0	17.8 ± 0.6	15.5 ± 1.0	19.8 ± 1.1
	BBear	16.2 ± 0.9	18.6 ± 0.6	16.4 ± 1.0	20.4 ± 1.0
	Kiamichi	17.0 ± 0.8	19.1 ± 0.6	17.1 ± 1.0	21.1 ± 0.9
MAP	Washita	615.6 ± 159.1	577.2 ± 147.8	608.7 ± 146.3	567.1 ± 162.7
	BBear	919.7 ± 224.8	883.9 ± 198.6	894.1 ± 192.8	817.3 ± 220.5
	Kiamichi	1326.4 ± 252.8	1302.4 ± 270.8	1291.9 ± 235.4	1300.1 ± 267.5

Table 4
Changes in ET (ΔET) and runoff (ΔR) (mm/year) per 1 % increase in tree cover of the total watershed area for Washita, BBear, and Kiamichi watersheds in the present and future periods under the RCP45 and RCP85 scenarios: Baseline vs. Forest+ comparisons. Values after ± symbol represent standard deviations, denoting annual variability for the entire simulated period.

		RCP45		RCP85	
		1991–2020	2070–2099	1991–2020	2070–2099
ΔET	Washita	0.41 ± 1.32	0.15 ± 1.07	0.36 ± 1.44	0.14 ± 1.07
	BBear	2.91 ± 1.01	2.30 ± 0.71	2.77 ± 1.04	1.88 ± 1.10
	Kiamichi	2.33 ± 0.69	2.35 ± 0.52	2.27 ± 0.72	2.41 ± 0.60
ΔR	Washita	−0.07 ± 0.12	−0.04 ± 0.10	−0.06 ± 0.12	−0.02 ± 0.04
	BBear	−1.79 ± 0.96	−1.29 ± 0.69	−1.65 ± 0.77	−1.08 ± 0.80
	Kiamichi	−1.08 ± 0.62	−1.06 ± 0.58	−0.98 ± 0.60	−1.10 ± 0.59

3.2. SWAT+ output

3.2.1. Watershed ET and runoff

In general, the effects of increasing tree cover on watershed ET and runoff varied among the climate conditions (Table 4 and S1). For each 1 % increase in tree cover, the subhumid BBear region had the greatest increase in ET (ΔET) and the corresponding reduction in runoff (ΔR) across the majority of scenarios. This was followed by the humid Kiamichi area and the semiarid Washita region. Specifically, during 1991–2020 under RCP45, BBear had the largest increase in ET at 2.91 mm/year per 1 % increase in tree cover. Conversely, during 2070–2099 under RCP85, Washita had the smallest increase in ET at 0.15 mm/year. Notably, both Washita and BBear were projected to experience considerably smaller increases in ET during 2070–2099 compared to the historical period of 1991–2020 under both RCP45 and RCP85 scenarios. In contrast, Kiamichi showed an opposite trend. These trends are inversely mirrored for changes in ΔR wherein the greatest decrease in ΔR in BBear and Washita aligned with the greatest increase in ΔET. The only exception occurred in Kiamichi, where ΔR increased from 1991 to 2020 to 2070–2099 in RCP45 but decreased in RCP85.

3.2.2. Blue water flow

Among the three watersheds, both climate change scenarios and an increase in tree cover generally led to a reduction of blue water flow. The only exception was for the Washita watershed, where a small increase in blue water flow could occur with increased tree cover under the RCP85 by the end of the 21st century. Under the Forest+ scenario, the Kiamichi watershed exhibited a relatively modest decrease in blue water flow (<10 %), while Washita and BBear watersheds were predicted to experience substantially greater percentage decreases in blue water flow (71.3 % and 32.3 %, respectively, Fig. 3), resulting in a loss of 32.5 mm/year and 250.3 mm/year on average (Table S1). Notably, the 250.3 mm/year decrease in BBear was the largest decrease in absolute values and the 32.5 mm/year decrease in Washita resulted in the depletion of soil water storage in some years (Tables S2 and S3).

3.2.3. Net primary productivity

Responses of NPP (ΔNPP) to Forest+ under both climate change scenarios differed among the three climate zones (Fig. 4 and Table S1). During the 1991–2020 period, BBear showed the greatest increase at 0.19 Mg/ha/year in NPP for every 1 % increase in tree cover across the watershed area, followed by Kiamichi and then Washita in both climate change scenarios. However, from 2070 to 2099, the increase in NPP for every 1 % increase in tree cover across the watershed area in BBear and Washita was projected to be lower than that projected for 1991–2020 period. The NPP increase in Washita during the 2070–2099 period under both climate scenarios was expected to be only about 30 % of that during 1991–2020. In contrast, ΔNPP slightly increased in Kiamichi compared to the period from 1991 to 2020, with the increase being greater in RCP45 than in RCP85.

3.2.4. Ecosystem water use efficiency at the watershed-scale

WUE across the three watersheds exhibited a discernible V-shaped trend along the climate gradient, regardless of the increase in forest cover and climate change scenarios (Fig. 5 and Table S4). For Baseline under both RCP45 and RCP85 scenarios, Kiamichi had the greatest WUE (16.98 and 16.00 kg/ha/mm, respectively), and remained similar until the end of the 21st century. WUE increased for Forest+ in Kiamichi by a similar amount between RCP45 and RCP85. BBear had the lowest WUE for all time periods but experienced a substantial surge of 169.5 % on average from Baseline to Forest+, marking the largest increase among all three watersheds for an equivalent increase in tree cover. During the period from 1991 to 2020 under both RCP45 and RCP85, Washita would have an approximately 15 kg/ha/mm improvement in WUE with increasing tree cover. However, this gain will reduce to around 6 kg/ha/mm during the period from 2070 to 2099.

4. Discussion

4.1. Ecosystem and climate interactions

In our study, we conducted simulations to assess the water budget and carbon gain (NPP) across three distinct watersheds situated in different climate zones along the climate gradient within the SGP. Overall, our hypotheses were supported by the results, albeit with a few exceptions. Specifically, Hypothesis (1) that increasing tree cover and

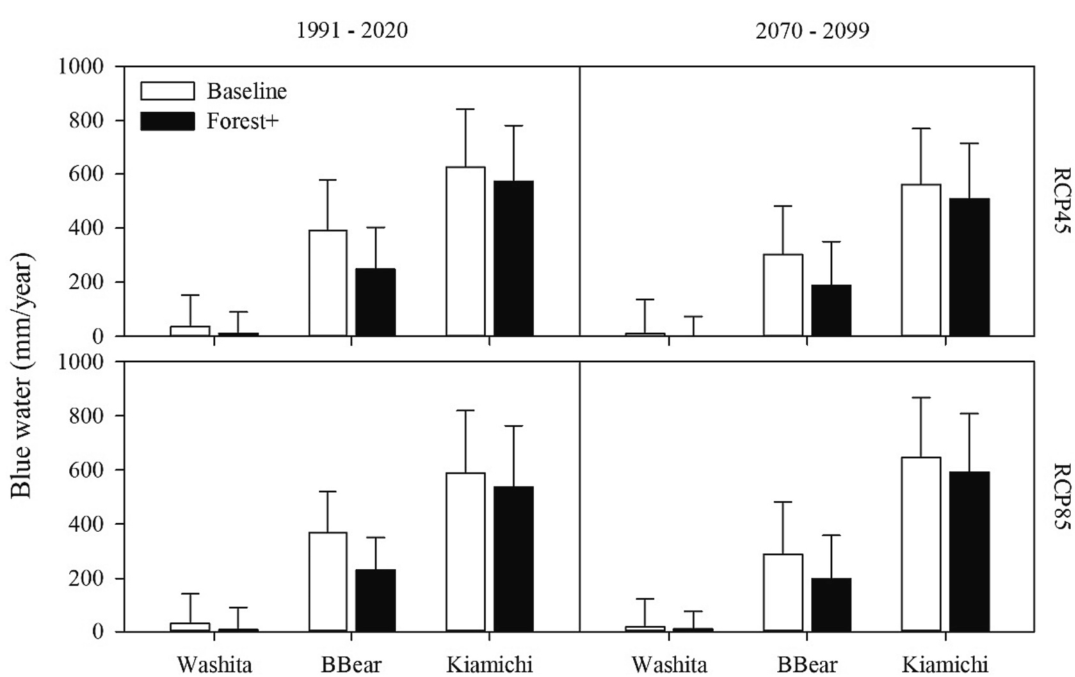

Fig. 3. Blue water depth (mm) in Washita, BBear, and Kiamichi under historic and future climate conditions simulated by the RCP45 and the RCP85 scenarios. Bars represent standard deviations, denoting annual variability for the entire simulated period.

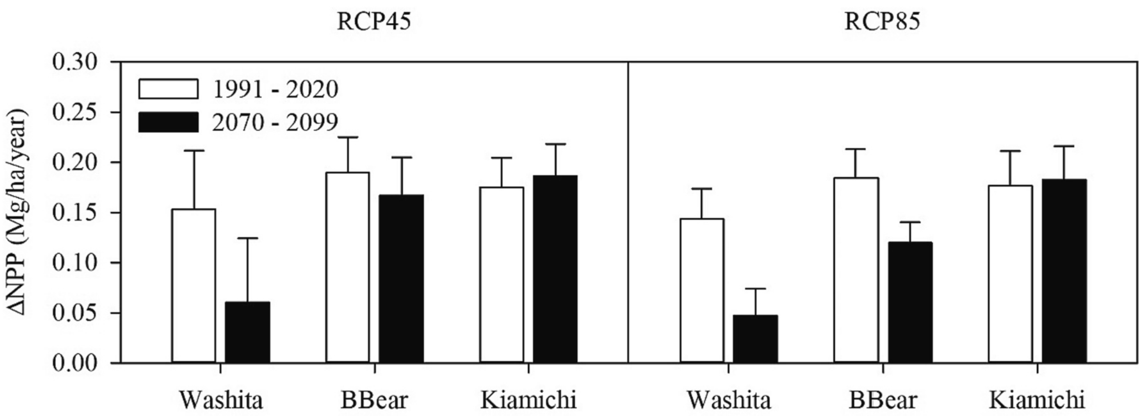

Fig. 4. Changes in NPP (net primary productivity, ΔNPP, Mg/ha/year) with a 1 % increase of total watershed area in tree cover between baseline and Forest+ in Washita, BBear, and Kiamichi under future climate conditions simulated by the RCP45 and the RCP85 scenarios. Bars represent standard deviations of ΔNPP for the entire simulated period.

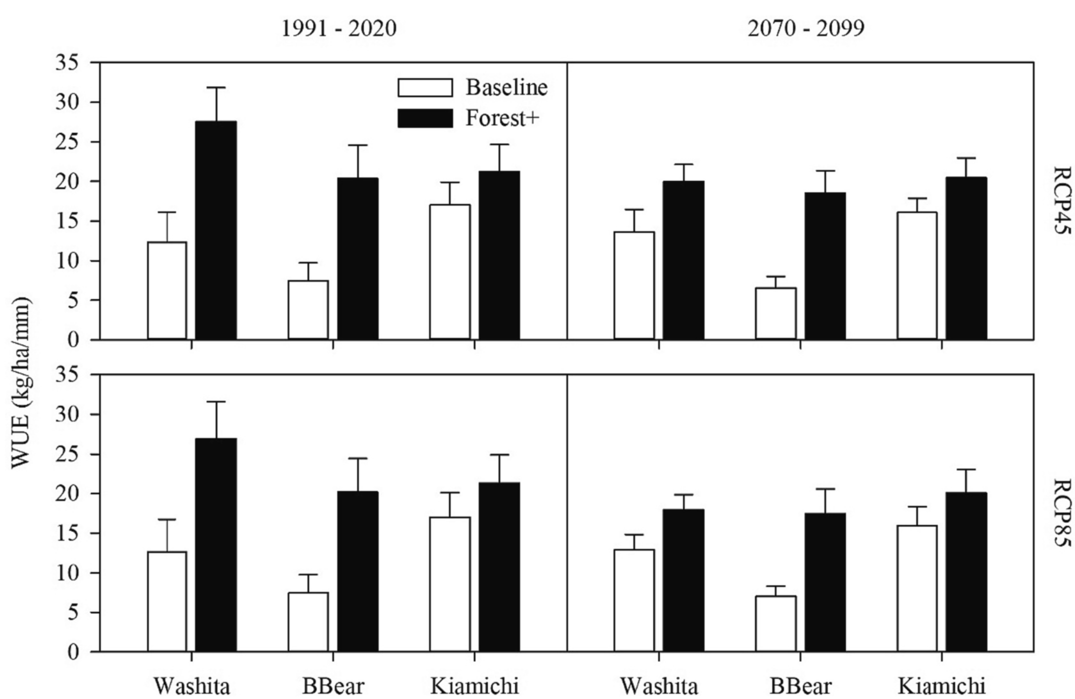

Fig. 5. Ecosystem water use efficiency (WUE) in Washita, BBear, and Kiamichi under historic and future climate conditions simulated by the RCP45 and the RCP85 scenarios. Bars represent standard deviations of WUE for the entire simulated period.

future climate change will elevate vegetation water use and reduce water yield held true when considering the impacts of increasing woody cover and climate change independently (Domke et al., 2020; Starks and Moriasi, 2017; Tölgyesi et al., 2023; Zou et al., 2018). However, when these factors were examined in conjunction, we observed a decreasing trend in vegetation water use in two of six comparisons of ET. The decrease in water use primarily stems from the projected decline in annual precipitation in both Washita and BBear (Table 3), leading to a reduction in total ET, despite an increase in annual temperature. Our Hypothesis (2) that increasing tree cover will increase ecosystem NPP, especially in a more humid climate than in a drier climate was not fully supported. While NPP increased with the increase of tree cover, the model projected the largest increase in the subhumid BBear and the smallest increase in the humid Kiamichi. This suggests that, in comparison to the humid region where tree cover is already high, an increase in tree cover in semiarid and subhumid regions will have a proportionally greater impact on NPP (Barger et al., 2011; O'Donnell and Caylor, 2012). Hypothesis (3) that the capacity of NPP associated with tree cover increase will decrease under future climate scenarios was generally upheld, except for Kiamichi under the RCP85 Forest+ scenario. This indicates that total precipitation may be a driving force of NPP, even though this relationship may not always be directly proportional (Mátyás and Sun, 2014; Tölgyesi et al., 2023). The complexities observed in these scenarios highlighted the critical need for a comprehensive understanding of the complex interactions between woody cover, climate change, and ecosystem carbon and water dynamics across various climatical regions.

4.2. Impacts of naturally increasing woody cover

The semiarid Washita watershed and the subhumid BBear watershed are undergoing a natural increase in evergreen tree cover as a result of eastern redcedar encroachment into both grasslands and oak woodlands (Wang et al., 2017; Zou et al., 2018). The simulated results from this study provide insights regarding the impact of WPE on both NPP and water use. However, there are some distinctions between naturally driven WPE and afforestation using planted trees. Woody plant expansion into grasslands is diffuse and patchy in the SGP (Archer, 1989). In semiarid watersheds, the distribution of woody cover from WPE is often controlled by soils and topography, which dictate how water is distributed and utilized (Browning et al., 2008). With the progression of future climate change, global temperature increases are anticipated, accompanied by a mixed pattern of precipitation trends across different regions in the SGP. This poses a challenge in predicting the extent of WPE or assessing habitat suitability for afforestation (Yang et al., 2024). Our model simulation indicated a substantial reduction in soil water content in successive years in Washita under the Forest+ scenarios for both RCP45 and RCP85 (Table S3). This suggests that plantation would lead to excessive soil moisture depletion and these conditions could even lead to larger scale mortality events within the plantation. It is likely that, due to climate conditions as well as the soil water withdrawal, a 100 % conifer cover in the Washita watershed may not be achievable or sustainable, whether through WPE or afforestation efforts (Archer et al., 2017; Sankaran et al., 2005). Nevertheless, this study conducted simulations considering a scenario where all grassland is converted to conifer forest, aiming to investigate how alteration in woody cover might impact the water budget and carbon gain in drier areas. This result represents the upper threshold for the potential gains in NPP and water use under changing climatic conditions.

In general, trees excel in carbon sequestration compared to grasses due to their greater biomass and extended lifespan. However, our simulations showed that increasing woody cover does not consistently lead to a proportional increase in net primary productivity. In Washita, BBear, and Kiamichi, a substantial increase in woody cover by factors of 52.3, 4.8, and 1.3 corresponded to NPP increases by 2.3-fold, 3.5-fold, and 1.3-fold, respectively. Only for Kiamichi did increased woody cover yield a similar NPP compared to the baseline scenario. Conversely, in Washita and BBear, the increase in woody cover resulted in a relatively smaller increase in NPP relative to the magnitude of the increase in woody cover. Webb et al. (1978) found that despite an increase in ET from 500 to 1000 mm/year, aboveground NPP remained relatively constant at approximately 8 Mg/ha/year in forests. This implies that in water-limited environments, to maintain productivity, forests tend to use more soil water and/or increase WUE, although it may be similar to the WUE in grasslands (Schmidt et al., 2021). However, the upper limit of ET and soil water content are primarily dictated by the amount and timing of precipitation. With extended drought often seen in the drier areas, this could further decrease blue water availability as suggested by our results. It is essential to note that despite the greater carbon storage of trees, the increase in woody cover did not consistently lead to a proportional enhancement in NPP in the studied regions. The availability of water typically emerges as the constraining factor in generating greater NPP, which implies that a high woody cover in water-limited areas may entail a suboptimal trade-off between carbon accrual and water utilization.

A notable concern raised from this study was the substantial increase of ET simulated in BBear under the Forest+ scenario. Subhumid areas, typically conducive to tree growth, offer favorable conditions for afforestation aimed at increasing atmospheric carbon sequestration (Griscom et al., 2017). However, our results showed an increase of approximately 270 mm in ET following the conversion of the entire grassland of BBear watershed into an evergreen forest. This implies the potential larger impact of land use change than climate change on water balance (Schreiner-McGraw et al., 2020). Consistent with the findings of Zhang et al. (2001), the annual ET differential between pasture and forest can exceed 200 mm in regions with annual precipitation of 900 mm. Additionally, Caterina et al. (2014) conducted a study in a nearby area and found that juniper woodland may utilize as much as 95 % of the total rainfall. These studies collectively offer compelling evidence that in the climate transition zone, such as the SGP, transitioning from grassland to evergreen forest can exert notable impacts on the water cycle, resulting in a substantial reduction in runoff and groundwater recharge. This also implies that controlling WPE in its early stage through prescribed burns and targeted herbicide applications to specific species might be more cost-effective and require less labor (Wilcox et al., 2018; Ansley and Castellano, 2006). To gain further insights into the carbon gain and water use trade-off, future studies will necessitate in situ measurement, including the application of techniques such as eddy covariance (Baldocchi, 2003; Burba, 2013).

4.3. Impacts of climate change

The study region is situated in the climate transition zone of the SGP, USA and is highly vulnerable to the impacts of climate change (Seager et al., 2018). As temperatures rise, evaporation and transpiration rates increase. In addition, precipitation is predicted to decrease, leading to reduced soil water for vegetation within our study regions, culminating in the eastward movement of drier climate conditions. Historically, the 100th meridian was considered the divide between the semi-arid and subhumid climate regions, which passes through the Washita watershed. However, due to decades of global warming, this divide has shifted east approaching the 98th meridian (Seager et al., 2018), which lies just west of the BBear watershed at present (Fig. S4). Consequently, even in regions experiencing increased precipitation, there could be a decline in the rate of photosynthesis (Hueve et al., 2011). This raises critical concerns about the efficacy of afforestation, as well as the early survival of seedlings, as a strategy for mitigating global warming, particularly if substantial temperature increases persist (Will et al., 2013). Additionally, increasing woody cover to enhance carbon sequestration often requires a greater consumption of water (Caterina et al., 2014; Yang et al., 2019). Our results indicate that although Washita may lose the majority of its blue water under the Forest+ scenario, the absolute amount lost is much smaller than BBear. This discrepancy may be attributed to the initially low blue water availability under the baseline scenario. It is also imperative to recognize that BBear is situated in an ecosystem transition zone, characterized by comparatively low ecosystem stability in contrast to the other two watersheds. Trabucco et al. (2008) reported a similar impact of afforestation/reforestation, wherein the reduction in runoff ranged from 15 % in humid areas to 54 % in drier areas. In water-limited regions, it is essential to explore alternative strategies for climate change mitigation, emphasizing the conservation of water resources and the preservation of existing ecosystems.

In this study, we selected the RCP45 and RCP85 climate scenarios due to the prevailing prediction of warmer and drier climates by most climate models. While cooler and wetter climate scenarios are also projected in other climate models, they are less common. It is imperative to acknowledge that climate models undergo continuous refinement, incorporating new data and insights from ongoing scientific studies. While this project was underway, the climate projections from CMIP6 became available. However, to meet the data input specifications for SWAT+, we opted to use the dataset from CMIP5 projections. This decision was made because downscaled and bias-corrected data with a spatial resolution of 4 km or higher were not yet available from the CMIP6 dataset. Thus, integrating the latest climate change projections is essential in assessing strategies to enhance carbon storage and conserve water.

4.4. Limitations of the study

Climate conditions in the three watersheds have considerable variations with a difference in MAP of almost 700 mm between Washita and Kiamichi. This wide range of climate conditions posed challenges for the SWAT+ simulations. A clear trend of improved model performance was observed from the semi-arid grassland to the humid forest. Although the SWAT+ is a relatively newer model, comparisons between the SWAT+ and the older SWAT indicated that the two models had similar performance (Her and Jeong, 2018; Kakarndee and Kositsakulchai, 2020) mostly because they share the same core model. Many studies also reported relatively low indices (e.g., NSE) in arid and semi-arid areas compared to humid regions (Ashraf Vaghefi et al., 2014; Qi et al., 2017; Tan et al., 2020; Tzoraki et al., 2013). This discrepancy could potentially arise from limitations in simulating certain soil hydrological characteristics, such as water conductivity in macropores, as well as the possibility of less accurate simulations in upper stream areas, where there are fewer observation stations to adequately represent the complex landscape and climate variations (Wu et al., 2022). Another potential contributing factor could be greater water use for irrigation in the drier regions (Zaussinger et al., 2019). In recent years, most states in the USA have seen an increase in total water withdrawal for irrigation (Das Bhowmik et al., 2020). Irrigation could add water to the natural cycle, change crop phenology, and introduce bias in SWAT modeling works in watersheds with significant irrigated agriculture (Marek et al., 2017). Addressing and improving the simulation results in the upper Washita River represents a potential area for future research, allowing a more accurate assessment of how land use and climate change might affect the water cycle and carbon storage in a drier area.

5. Conclusions

In this study, we simulated the impacts of a 100 % conversion of rangeland into evergreen forest on ecosystem water dynamics and productivity in three watersheds along the climate gradient in the SGP. Our findings indicate that both climate change and increased woody cover are linked with a reduction in water resources in most cases, with drier regions experiencing more pronounced effects. However, the combined effect of afforestation and climate change was not simply additive. Drier watersheds, particularly the watersheds in the climate transition zones, may experience greater loss of runoff than wetter regions. Furthermore, augmenting tree cover in regions already dominated by trees (through restocking) will indeed elevate carbon sequestration levels, albeit with a relatively lower increase in water use efficiency. Although our study is regionally centered on the SGP, these insights can be applied globally. The phenomena of afforestation and WPE are widespread, and our findings are crucial in comprehending their effects on ecosystems under similar climate gradients worldwide. This highlights the imperative for broader research to corroborate these results across diverse geographical contexts. A strong correlation exists between simulated increases in woody cover, ET, and reduced availability of blue water across all studied watersheds. These findings highlight the complex interactions among woody cover, ecosystem productivity, and water use, underscoring the need for further research to better comprehend and manage these dynamics for effective carbon mitigation strategies. Afforestation and reforestation in drier areas may lead to large water loss for urban, agricultural, and aquatic ecosystems and such endeavors should be approached with caution and generally not encouraged. Conversely, reforestation initiatives in humid regions hold promise for carbon sequestration although the benefits might be less pronounced in areas where tree cover is already extensive. Consequently, practices aimed at carbon sequestration through afforestation should be carefully evaluated, taking into account specific climate zones and climate change scenarios, to optimize carbon sequestration while avoiding potential exacerbation of water scarcity, particularly in regions where there is a high demand for blue water resources.

CRediT authorship contribution statement

Tian Zhang: Writing – original draft, Investigation, Conceptualization. **Jia Yang:** Writing – review & editing. **Abigail Winrich:** Writing – review & editing. **Rodney E. Will:** Writing – review & editing, Funding acquisition. **Chris B. Zou:** Writing – review & editing, Funding acquisition, Conceptualization.

Declaration of competing interest

The authors declare that they have no known competing financial interests or personal relationships that could have appeared to influence the work reported in this paper.

Data availability

Data will be made available on request.

Acknowledgments

Oklahoma NSF EPSCoR provides funding support for the work under Grant No. OIA-1946093. The support from Oklahoma Agricultural Experiment Station, McIntire Stennis OKL03151 and OKL03152, and the endowment for the Sarkeys Distinguished Professorship is gratefully acknowledged. The authors would like to thank Ms. Nancy Sammons for her technical assistance in conducting the SWAT+ model simulations.

Appendix A. Supplementary data

Supplementary data to this article can be found online at https://doi.org/10.1016/j.scitotenv.2024.170255.

References

Abatzoglou, J.T., 2013. Development of gridded surface meteorological data for ecological applications and modelling. Int. J. Climatol. 33 (1), 121–131.
Abbaspour, K.C., Rouholahnejad, E., Vaghefi, S., Srinivasan, R., Yang, H., Kløve, B., 2015. A continental-scale hydrology and water quality model for Europe: calibration and uncertainty of a high-resolution large-scale SWAT model. J. Hydrol. 524, 733–752.
Adane, Z.A., Nasta, P., Zlotnik, V., Wedin, D., 2018. Impact of grassland conversion to forest on groundwater recharge in the Nebraska Sand Hills. Journal of Hydrology: Regional Studies 15, 171–183.
Ameray, A., Bergeron, Y., Valeria, O., Montoro Girona, M., Cavard, X., 2021. Forest carbon management: a review of silvicultural practices and management strategies across boreal, temperate and tropical forests. Current Forestry Reports 1–22.
Ansley, R.J., Castellano, M.J., 2006. Strategies for savanna restoration in the southern Great Plains: effects of fire and herbicides. Restor. Ecol. 14 (3), 420–428.
Ansley, R.J., Wu, X.B., Kramp, B.A., 2001. Observation: long-term increases in mesquite canopy cover in a North Texas savanna. J. Range Manage. 54 (2), 171–176.
Archer, S., 1989. Have southern Texas savannas been converted to woodlands in recent history? Am. Nat. 134 (4), 545–561.
Archer, S., Schimel, D.S., Holland, E.A., 1995. Mechanisms of shrubland expansion: land use, climate or CO_2? Clim. Change 29 (1), 91–99.
Archer, S.R., Andersen, E.M., Predick, K.I., Schwinning, S., Steidl, R.J., Woods, S.R., 2017. Woody Plant Encroachment: Causes and Consequences. Processes, Management and Challenges, Rangeland Systems, pp. 25–84.
Arnold, J.G., Fohrer, N., 2005. SWAT2000: current capabilities and research opportunities in applied watershed modelling. Hydrol. Process. 19 (3), 563–572.
Ashraf Vaghefi, S., Mousavi, S.J., Abbaspour, K.C., Srinivasan, R., Yang, H., 2014. Analyses of the impact of climate change on water resources components, drought and wheat yield in semiarid regions: Karkheh River basin in Iran. Hydrol. Process. 28 (4), 2018–2032.
Asner, G.P., Archer, S., Hughes, R.F., Ansley, R.J., Wessman, C.A., 2003. Net changes in regional woody vegetation cover and carbon storage in Texas drylands, 1937–1999. Glob. Chang. Biol. 9 (3), 316–335.
Bala, G., Caldeira, K., Wickett, M., Phillips, T.J., Lobell, D.B., Delire, C., Mirin, A., 2007. Combined climate and carbon-cycle effects of large-scale deforestation. Proc. Natl. Acad. Sci. 104 (16), 6550–6555.
Baldocchi, D.D., 2003. Assessing the eddy covariance technique for evaluating carbon dioxide exchange rates of ecosystems: past, present and future. Glob. Chang. Biol. 9 (4), 479–492.
Barger, N.N., Archer, S.R., Campbell, J.L., Huang, C.Y., Morton, J.A., Knapp, A.K., 2011. Woody plant proliferation in north American drylands: a synthesis of impacts on ecosystem carbon balance. J. Geophys. Res. Biogeo. 116 (G4).
Bieger, K., Arnold, J.G., Rathjens, H., White, M.J., Bosch, D.D., Allen, P.M., Volk, M., Srinivasan, R., 2017. Introduction to SWAT+, a completely restructured version of the soil and water assessment tool. JAWRA Journal of the American Water Resources Association 53 (1), 115–130.
Bigelow, D., Borchers, A., 2017. Major uses of land in the United States, 2012 (no. 1476-2017-4340).
Bonan, G.B., 2008. Forests and climate change: forcings, feedbacks, and the climate benefits of forests. Science 320 (5882), 1444–1449.
Briggs, J.M., Knapp, A.K., Brock, B.L., 2002. Expansion of woody plants in tallgrass prairie: a fifteen-year study of fire and fire-grazing interactions. Am. Midl. Nat. 147 (2), 287–294.

Browning, D.M., Archer, S.R., Asner, G.P., McClaran, M.P., Wessman, C.A., 2008. Woody plants in grasslands: post-encroachment stand dynamics. Ecol. Appl. 18 (4), 928–944.

Burba, G., 2013. Eddy Covariance Method for Scientific, Industrial, Agricultural and Regulatory Applications: A Field Book on Measuring Ecosystem Gas Exchange and Areal Emission Rates. LI-Cor Biosciences.

Caterina, G.L., Will, R.E., Turton, D.J., Wilson, D.S., Zou, C.B., 2014. Water use of Juniperus virginiana trees encroached into Mesic prairies in Oklahoma, USA. Ecohydrology 7 (4), 1124–1134.

Chausson, A., Turner, B., Seddon, D., Chabaneix, N., Girardin, C.A., Kapos, V., Key, I., Roe, D., Smith, A., Woroniecki, S., Seddon, N., 2020. Mapping the effectiveness of nature-based solutions for climate change adaptation. Glob. Chang. Biol. 26 (11), 6134–6155.

Das Bhowmik, R., Seo, S.B., Das, P., Sankarasubramanian, A., 2020. Synthesis of irrigation water use in the United States: spatiotemporal patterns. J. Water Resour. Plan. Manag. 146 (7), 04020050.

Di Sacco, A., Hardwick, K.A., Blakesley, D., Brancalion, P.H., Breman, E., Cecilio Rebola, L., Chomba, S., Dixon, K., Elliott, S., Ruyonga, G., Shaw, K., 2021. Ten golden rules for reforestation to optimize carbon sequestration, biodiversity recovery and livelihood benefits. Glob. Chang. Biol. 27 (7), 1328–1348.

Domke, G.M., Oswalt, S.N., Walters, B.F., Morin, R.S., 2020. Tree planting has the potential to increase carbon sequestration capacity of forests in the United States. Proc. Natl. Acad. Sci. 117 (40), 24649–24651.

Eldridge, D.J., Bowker, M.A., Maestre, F.T., Roger, E., Reynolds, J.F., Whitford, W.G., 2011. Impacts of shrub encroachment on ecosystem structure and functioning: towards a global synthesis. Ecol. Lett. 14 (7), 709–722.

Falkenmark, M., 1995. Land-water linkages: a synopsis. FAO Land and Water Bulletin 1, 15–17.

Farr, T.G., Rosen, P.A., Caro, E., Crippen, R., Duren, R., Hensley, S., Kobrick, M., Paller, M., Rodriguez, E., Roth, L., Seal, D., 2007. The shuttle radar topography mission. Rev. Geophys. 45 (2).

Gardner, R., 2009. Trees as technology: planting shelterbelts on the Great Plains. Hist. Technol. 25 (4), 325–341.

Gent, P.R., Danabasoglu, G., Donner, L.J., Holland, M.M., Hunke, E.C., Jayne, S.R., Lawrence, D.M., Neale, R.B., Rasch, P.J., Vertenstein, M., Worley, P.H., 2011. The community climate system model version 4. J. Climate 24 (19), 4973–4991.

Griscom, B.W., Adams, J., Ellis, P.W., Houghton, R.A., Lomax, G., Miteva, D.A., Schlesinger, W.H., Shoch, D., Siikamäki, J.V., Smith, P., Woodbury, P., 2017. Natural climate solutions. Proc. Natl. Acad. Sci. 114 (44), 11645–11650.

Her, Y., Jeong, J., 2018. SWAT+ versus SWAT2012: comparison of sub-daily urban runoff simulations. Transactions of the ASABE 61 (4), 1287–1295.

Hoek van Dijke, A.J., Herold, M., Mallick, K., Benedict, I., Machwitz, M., Schlerf, M., Pranindita, A., Theeuwen, J.J., Bastin, J.F., Teuling, A.J., 2022. Shifts in regional water availability due to global tree restoration. Nat. Geosci. 15 (5), 363–368.

Homer, C., Huang, C., Yang, L., Wylie, B., Coan, M., 2004. Development of a 2001 national land-cover database for the United States. Photogramm. Eng. Remote Sens. 70 (7), 829–840.

Hueve, K., Bichele, I., Rasulov, B., Niinemets, Ü.L.O., 2011. When it is too hot for photosynthesis: heat-induced instability of photosynthesis in relation to respiratory burst, cell permeability changes and H2O2 formation. Plant Cell Environ. 34 (1), 113–126.

Huxman, T.E., Wilcox, B.P., Breshears, D.D., Scott, R.L., Snyder, K.A., Small, E.E., Hultine, K., Pockman, W.T., Jackson, R.B., 2005. Ecohydrological implications of woody plant encroachment. Ecology 86 (2), 308–319.

Joffre, R., Rambal, S., 1993. How tree cover influences the water balance of Mediterranean rangelands. Ecology 74 (2), 570–582.

Kakarndee, I., Kositsakulchai, E., 2020. Comparison between SWAT and SWAT+ for simulating streamflow in a paddy-field-dominated basin, Northeast Thailand. In: E3S Web of Conferences, vol. 187. EDP Sciences, p. 06002.

Kishawi, Y., Mittelstet, A.R., Gilmore, T.E., Twidwell, D., Roy, T., Shrestha, N., 2023. Impact of eastern Redcedar encroachment on water resources in the Nebraska Sandhills. Sci. Total Environ. 858, 159696.

Kulmatiski, A., Beard, K.H., 2013. Woody plant encroachment facilitated by increased precipitation intensity. Nat. Clim. Chang. 3 (9), 833–837.

Lal, R., 2008. Sequestration of atmospheric CO_2 in global carbon pools. Energ. Environ. Sci. 1 (1), 86–100.

Li, L., Hosseiniaghdam, E., Drijber, R., Jeske, E., Awada, T., Hiller, J., Kaiser, M., 2023. Conversion of native grassland to coniferous forests decreased stocks of soil organic carbon and microbial biomass. Plant and Soil 1–14.

Marek, G.W., Gowda, P.H., Marek, T.H., Porter, D.O., Baumhardt, R.L., Brauer, D.K., 2017. Modeling long-term water use of irrigated cropping rotations in the Texas High Plains using SWAT. Irrig. Sci. 35, 111–123.

Masson-Delmotte, V., Zhai, P., Pirani, A., Connors, S.L., Péan, C., Berger, S., Caud, N., Chen, Y., Goldfarb, L., Gomis, M.I., Huang, M., 2021. Climate change 2021: The physical science basis. In: Contribution of Working Group I to the Sixth Assessment Report of the Intergovernmental Panel on Climate Change. Cambridge University Press, Cambridge, United Kingdom and New York, NY, USA.

Mátyás, C., Sun, G., 2014. Forests in a water limited world under climate change. Environ. Res. Lett. 9 (8), 085001.

Morgan, J.A., Follett, R.F., Allen, L.H., Del Grosso, S., Derner, J.D., Dijkstra, F., Franzluebbers, A., Fry, R., Paustian, K., Schoeneberger, M.M., 2010. Carbon sequestration in agricultural lands of the United States. J. Soil Water Conserv. 65 (1), 6A–13A.

Moriasi, D.N., Arnold, J.G., Van Liew, M.W., Bingner, R.L., Harmel, R.D., Veith, T.L., 2007. Model evaluation guidelines for systematic quantification of accuracy in watershed simulations. Trans. ASABE 50 (3), 885–900.

Mykleby, P.M., Snyder, P.K., Twine, T.E., 2017. Quantifying the trade-off between carbon sequestration and albedo in midlatitude and high-latitude north American forests. Geophys. Res. Lett. 44 (5), 2493–2501.

Niu, X., Duiker, S.W., 2006. Carbon sequestration potential by afforestation of marginal agricultural land in the Midwestern US. For. Ecol. Manage. 223 (1–3), 415–427.

Nosetto, M.D., Jobbágy, E.G., Paruelo, J.M., 2006. Carbon sequestration in semi-arid rangelands: comparison of Pinus ponderosa plantations and grazing exclusion in NW Patagonia. J. Arid Environ. 67 (1), 142–156.

O'Donnell, F.C., Caylor, K.K., 2012. A model-based evaluation of woody plant encroachment effects on coupled carbon and water cycles. J. Geophys. Res. Biogeo. 117 (G2).

Potts, D.L., Huxman, T.E., Cable, J.M., English, N.B., Ignace, D.D., Eilts, J.A., Mason, M. J., Weltzin, J.F., Williams, D.G., 2006. Antecedent moisture and seasonal precipitation influence the response of canopy-scale carbon and water exchange to rainfall pulses in a semi-arid grassland. New Phytol. 170 (4), 849–860.

Qi, Z., Kang, G., Chu, C., Qiu, Y., Xu, Z., Wang, Y., 2017. Comparison of SWAT and GWLF model simulation performance in humid south and semi-arid north of China. Water 9 (8), 567.

Qiao, L., Will, R., Wagner, K., Zhang, T., Zou, C., 2022. Improvement of evapotranspiration estimates for grasslands in the southern Great Plains: comparing a biophysical model (SWAT) and remote sensing (MODIS). Journal of Hydrology: Regional Studies 44, 101275.

Sankaran, M., Hanan, N.P., Scholes, R.J., Ratnam, J., Augustine, D.J., Cade, B.S., Gignoux, J., Higgins, S.I., Le Roux, X., Ludwig, F., Ardo, J., 2005. Determinants of woody cover in African savannas. Nature 438 (7069), 846–849.

Sauer, T.J., Wacha, K.M., Brevik, E.C., Zamora, D., 2023. Eastern red cedar effects on carbon sequestration and soil quality in the Great Plains. Soil Sci. Soc. Am. J. 87, 932–947.

Schmidt, K.N., Zou, C.B., Kakani, V.G., Zhong, Y., Will, R.E., 2021. Improved productivity, water yield, and water use efficiency by incorporating switchgrass cultivation and native ecosystems in an integrated biofuel feedstock system. GCB Bioenergy 13 (3), 369–381.

Schreiner-McGraw, A.P., Vivoni, E.R., Ajami, H., Sala, O.E., Throop, H.L., Peters, D.P., 2020. Woody Plant encroachment has a larger impact than climate change on dryland water budgets. Sci. Rep. 10 (1), 8112.

Schwärzel, K., Zhang, L., Montanarella, L., Wang, Y., Sun, G., 2020. How afforestation affects the water cycle in drylands: a process-based comparative analysis. Glob. Chang. Biol. 26 (2), 944–959.

Seager, R., Feldman, J., Lis, N., Ting, M., Williams, A.P., Nakamura, J., Liu, H., Henderson, N., 2018. Whither the 100th meridian? The once and future physical and human geography of America's arid-humid divide. Part II: the meridian moves east. Earth Interact. 22 (5), 1–24.

Starks, P.J., Moriasi, D.N., 2017. Impact of eastern redcedar encroachment on stream discharge in the North Canadian River basin. J. Soil Water Conserv. 72 (1), 12–25.

Tan, M.L., Gassman, P.W., Yang, X., Haywood, J., 2020. A review of SWAT applications, performance and future needs for simulation of hydro-climatic extremes. Adv. Water Resour. 143, 103662.

Tölgyesi, C., Hábenczyus, A.A., Kelemen, A., Török, P., Valkó, O., Deák, B., Erdős, L., Tóth, B., Csikós, N., Bátori, Z., 2023. How to not trade water for carbon with tree planting in water-limited temperate biomes? Sci. Total Environ. 856, 158960.

Torquato, P.R., Will, R.E., Zhang, B., Zou, C.B., 2020. Stand-level transpiration increases after eastern redcedar (Juniperus virginiana L.) encroachment into the midstory of oak forests. Forests 11 (9), 901.

Trabucco, A., Zomer, R.J., Bossio, D.A., van Straaten, O., Verchot, L.V., 2008. Climate change mitigation through afforestation/reforestation: a global analysis of hydrologic impacts with four case studies. Agr Ecosyst Environ 126 (1–2), 81–97.

Tyrl, R.J., Bidwell, T.G., Masters, R.E., Elmore, R.D., Weir, J.R., 2007. Oklahoma's native vegetation types. Oklahoma Cooperative Extension Service. https://extension.okstate.edu/fact-sheets/oklahomas-native-vegetation-types.html. (Accessed 23 December 2023).

Tzoraki, O., Cooper, D., Kjeldsen, T., Nikolaidis, N.P., Gamvroudis, C., Froebrich, J., Querner, E., Gallart, F., Karalemas, N., 2013. Flood generation and classification of a semi-arid intermittent flow watershed: Evrotas river. International Journal of River Basin Management 11 (1), 77–92.

U.S. Geological Survey., 2003. Aquifers: Map of the Principal Aquifers of the United States. https://water.usgs.gov/ogw/aquifer/map.html (accessed 4 January 2024).

Van Auken, O.W., 2009. Causes and consequences of woody plant encroachment into western north American grasslands. J. Environ. Manage. 90 (10), 2931–2942.

Wang, J., Xiao, X., Qin, Y., Dong, J., Geissler, G., Zhang, G., Cejda, N., Alikhani, B., Doughty, R.B., 2017. Mapping the dynamics of eastern redcedar encroachment into grasslands during 1984–2010 through PALSAR and time series Landsat images. Remote Sens. Environ. 190, 233–246.

Webb, W., Szarek, S., Lauenroth, W., Kinerson, R., Smith, M., 1978. Primary productivity and water use in native forest, grassland, and desert ecosystems. Ecology 59 (6), 1239–1247.

Wilcox, B.P., Huang, Y., 2010. Woody plant encroachment paradox: Rivers rebound as degraded grasslands convert to woodlands. Geophys. Res. Lett. 37 (7).

Wilcox, B.P., Birt, A., Archer, S.R., Fuhlendorf, S.D., Kreuter, U.P., Sorice, M.G., van Leeuwen, W.J., Zou, C.B., 2018. Viewing woody-plant encroachment through a social–ecological lens. BioScience 68 (9), 691–705.

Will, R.E., Wilson, S.M., Zou, C.B., Hennessey, T.C., 2013. Increased vapor pressure deficit due to higher temperature leads to greater transpiration and faster mortality during drought for tree seedlings common to the forest–grassland ecotone. New Phytol. 200 (2), 366–374.

Wine, M.L., Zou, C.B., 2012. Long-term streamflow relations with riparian gallery forest expansion into tallgrass prairie in the southern Great Plains, USA. For. Ecol. Manage. 266, 170–179.
Wu, L., Liu, X., Yang, Z., Yu, Y., Ma, X., 2022. Effects of single-and multi-site calibration strategies on hydrological model performance and parameter sensitivity of large-scale semi-arid and semi-humid watersheds. Hydrol. Process. 36 (6), e14616.
Yang, H., Rood, S.B., Flanagan, L.B., 2019. Controls on ecosystem water-use and water-use efficiency: insights from a comparison between grassland and riparian forest in the northern Great Plains. Agric. For. Meteorol. 271, 22–32.
Yang, J., Will, R., Zou, C., Zhai, L., Winrich, A., Fang, S., 2024. Eastward shift in Juniperus virginiana distribution range under future climate conditions in the southern Great Plains. United States. Agricultural and Forest Meteorology 345, 109836.
Zaussinger, F., Dorigo, W., Gruber, A., Tarpanelli, A., Filippucci, P., Brocca, L., 2019. Estimating irrigation water use over the contiguous United States by combining satellite and reanalysis soil moisture data. Hydrol. Earth Syst. Sci. 23 (2), 897–923.
Zhang, L., Walker, G.R., Dawes, W., 1999. Predicting the effect of vegetation changes on catchment average water balance. In: CRC for Catchment Hydrology, Technical Report 99/12. Monash University, Victoria, Australia.
Zhang, L., Dawes, W.R., Walker, G.R., 2001. Response of mean annual evapotranspiration to vegetation changes at catchment scale. Water Resour. Res. 37 (3), 701–708.
Zhang, M., Wei, X., 2021. Deforestation, forestation, and water supply. Science 371 (6533), 990–991.
Zomer, R.J., Xu, J., Trabucco, A., 2022. Version 3 of the global aridity index and potential evapotranspiration database. Scientific Data 9 (1), 409.
Zou, C.B., Turton, D.J., Will, R.E., Engle, D.M., Fuhlendorf, S.D., 2014. Alteration of hydrological processes and streamflow with juniper (*Juniperus virginiana*) encroachment in a mesic grassland catchment. Hydrol. Process. 28 (26), 6173–6182.
Zou, C.B., Twidwell, D., Bielski, C.H., Fogarty, D.T., Mittelstet, A.R., Starks, P.J., Will, R. E., Zhong, Y., Acharya, B.S., 2018. Impact of eastern redcedar proliferation on water resources in the Great Plains USA—current state of knowledge. Water 10 (12), 1768.